Controlling armchair and zigzag edges in oxidative cutting of graphene

Sk, Mahasin Alam; Huang, Lin; Chen, Peng; Lim, Kok Hwa

2016

Sk, M. A., Huang, L., Chen, P., & Lim, K. H. (2016). Controlling armchair and zigzag edges in oxidative cutting of graphene. Journal of Materials Chemistry C, 4(27), 6539-6545.

https://hdl.handle.net/10356/84815

https://doi.org/10.1039/C6TC01947A

Controlling armchair and zigzag edges in oxidative cutting of graphene†

Mahasin Alam Sk,[a] Lin Huang,[a] Peng Chen,[a,*] Kok Hwa Lim[b,*]

[a]*Division of Bioengineering, School of Chemical and Biomedical Engineering, Nanyang Technological University, 70 Nanyang Drive, 637457, Singapore*

[b]*Singapore Institute of Technology, 10 Dover Drive, 138683, Singapore*

Density-functional theory (DFT) calculations reveal that the formation of armchair epoxy chain on graphene sheet is energetically favorable when oxidation occurred on both sides of graphene sheet. However, the formation of zigzag epoxy chain is favorable when oxidation occurred on the same side of graphene sheet. In addition, the zigzag epoxy chain formation on graphene sheet becomes energetically more favorable when external strain is applied on graphene. Our theoretical calculations show that the edge (armchair or zigzag) of graphene nanoribbons (GNRs) and graphene quantum dots (GQDs) can be synthetically controlled by (a) experimental conditions which allow the oxidation of graphene to happen on either one or both sides of graphene sheet and (b) engineering the strain on graphene sheet.

*Corresponding author emails: chenpeng@ntu.edu.sg or KokHwa.Lim@SingaporeTech.edu.sg

† Electronic Supplementary Information (ESI) available: Equations for binding energy calculation, structures of oxidized graphene with one, two and three epoxy groups; binding energy of strained graphene.

1 Introduction

Graphene-based materials e.g., graphene nanoribbons (GNRs) and graphene quantum dots (GQDs), have attracted great attention of researchers after experimental report of graphene sheet by Novoselov et al. in 2004.[1] GNRs have potential applications in field effect transistors[2], gas- and bio- sensors[3, 4] and memory cells[5]. On the other hand GQDs have great potential in various applications such as bio-imaging and display[6-9], sensing[10,11], energy storage[12] and photovoltaics[13, 14]. It has been reported that GNRs with dominantly armchair edges have larger band gap as compared to similar sized GNRs with dominantly zigzag edges.[15] The origin of band gap in GNRs with armchair edges is attributed to both quantum confinement and crucial edge effect. However, the appearance of band gap in GNRs with zigzag edges is attributed to the staggered sub-lattice potential on hexagonal lattice due to edge magnetization.[16] Recent, theoretical calculations[17] from our group revealed that GQDs with armchair edges have different electronic and optical properties compared to similar sized GQDs with zigzag edges. It is evident that the edges of GNRs and GQDs control their electronic and optical properties. Therefore, it is essential to develop synthetic tools to control the edges of GNRs and GQDs to tailor for their applications.

The synthetic methods used for the production of GNRs and GQDs includes electron-beam lithography and plasma etching[18-22], sonochemical and electrochemical etching[23, 24], metal catalyzed cutting[25, 26], and reduction of exfoliated graphene oxide (hydrothermal method)[27, 28] and oxidation unzipping[29, 30]. However, no methods have been reported to be able to selectively produce GNRs and GQDs with either zigzag or armchair edge. Therefore, it is meaningful to

understand the cutting mechanism of graphene to control the edges of GNRs and GQDs. Numerous studies have been performed to explore the mechanism of oxidative unzipping of graphene both experimentally[31, 32] and theoretically[6, 13, 31, 33]. Li et al.[31] reported the occurrence of line defects on partially oxidized highly oriented pyrolytic graphite (HOPG) by examining the dark field optical microscope image. The strain generated by the cooperative alignment of epoxy groups is attributed to be the cause of cracking on graphite oxide (GO) using density-functional theory (DFT) calculations[31]. The formation of epoxy chain along zigzag orientation on same side of graphene sheet breaks the C-C bonds which are demonstrated by DFT calculations. This led to conclusion that the breaking of C-C bonds by formation of epoxy chain is responsible for the cutting of graphene sheet. In contrast, molecular dynamics simulations reported that breaking of underlying C-C bonds does not lead to cutting of the graphene sheet.[34] A two-steps mechanism of oxidative cutting of graphene sheet was proposed using DFT calculations by Li et al.[35] – (a) oxygen (O) atoms form epoxy pairs on both sides of graphene sheet and (b) then transformed to more stable carbonyl pairs which results in the breaking of graphene sheet. DFT calculations[36] also predicted that the oxidative cutting of graphene can form GNRs with large and controllable aspect ratios by applying external tensile strain. Alignments of epoxy chain on same side of graphene sheet along the zigzag orientation are considered (see Fig. 1) in most of the theoretical calculations.

In present study, we have performed systematic DFT calculations for the adsorption of O atoms to form epoxy groups on both sides of graphene planes. Our study reveals that the

formation of epoxy chains along armchair orientation (see Fig. 1) is energetically most favorable considering oxidation on both sides. The formation of zigzag epoxy chain becomes more favorable when external strain is applied on graphene sheet.

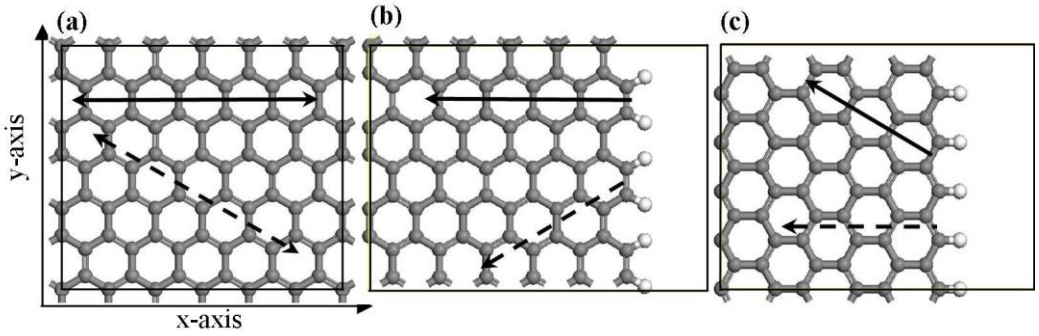

Fig. 1 The structural model of (a) 2D graphene; and 1D graphene with (b) armchair and (c) zigzag edges. The edge of graphene is terminated with H. Grey sphere – C atom, white sphere – H atom, solid arrow - zigzag epoxy chain and dotted arrow - armchair epoxy chain.

2 Computational models and methods

The oxidation of graphene is often done by treating graphene with oxidizing agents (e.g. solution of $KMnO_4$ in H_2SO_4). The generated oxygen leads to oxidation of graphene. Due to large size of graphene sheet, the oxidation process can initiate either from edge or middle of the graphene sheet. To model the oxidation at the middle part of graphene we have considered 2D periodic (x and y-directions) model of graphene (6x6) as shown in Fig. 1a. To study the oxidation at both armchair (Fig. 1b) and zigzag (Fig. 1c) edges of graphene, we used a 1D periodic (y-direction) models. The armchair and zigzag edges of graphene are passivated with H atoms (Fig. 1b-c) for edge-models. Adsorption of O atoms with graphene is used to model

graphene oxidation.

All the calculations are performed in the frame work of density functional theory (DFT) within the generalized gradient approximation (GGA) method using Perdew-Burke-Eznerhof (PBE) functional (GGA-PBE)[37] as implemented in Vienna ab initio simulation package (VASP).[38-40] The projector augmented wave method (PAW)[41, 42] is used to describe the interaction between the atomic cores and electrons. A 2×2×1 Monkhorst-Pack *k*-point[43] mesh and an energy cut of 450 eV are used for all calculations. The structure optimization is continued until the maximum forces acting on each atom become less than 0.01 eV $Å^{-1}$.

3 Results and discussion

Oxidation at basal plane of graphene

For the adsorption of O atom at middle part of graphene, only possible adsorption site is the carbon atoms at basal plane. The calculated binding energy of O atom on graphene is -2.41 eV in agreement to the reported value of -2.4 eV[31] on coronene molecule by Li et al.[31] They have studied the epoxy chain formation on the same side of coronene because one side of graphene sheet is usually accessible to oxidation due to experimental conditions e.g., usually one side of graphene is accessible for oxidation in graphite[29, 44]. This is likely the reason that the subsequent theoretical studies focused on same side oxidation of graphene.[16, 36] However, Schniepp et al. reported that it is possible to obtain epoxy functional groups on both side of graphene by treating graphite in an oxidizing solution.[45] Here, we use the adsorption of O atoms on both sides of

graphene sheet as the model for the formation of epoxy groups on both sides of graphene sheet[35] as reported by Schniepp et. al.[45]. We also consider the binding sites near to the pre-adsorbed O atom for subsequent O atoms adsorption (see Fig. S1-3) as the adsorption of O atom on oxidized graphene prefers carbon atoms with nearby oxygen[31].

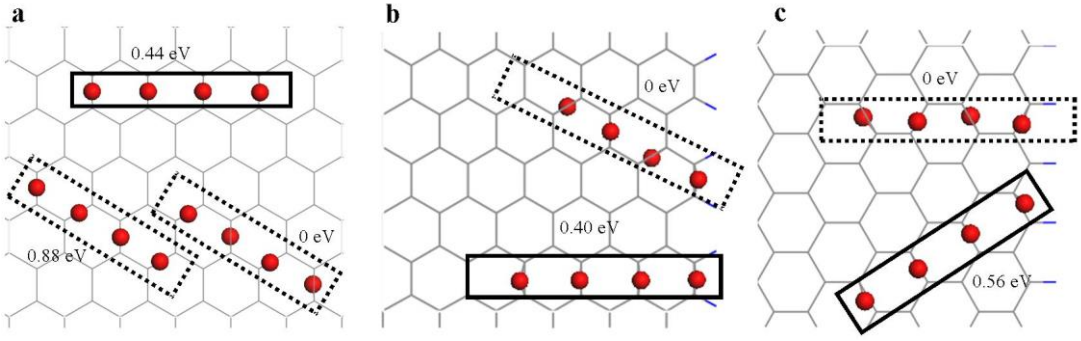

Fig. 2 Epoxy chain formation along armchair and zigzag orientation at (a) middle and (b-c) edge part of graphene. The value in eV is the relative energy. Grey stick – C atom and blue stick – H atom.

To study the formation of second epoxy group on graphene, we have considered five binding sites (Fig. S2). Our calculations show that the formation of second epoxy group along armchair orientation but on opposite side of the pre-adsorbed O atom is energetically most favorable (Fig. S2d). Our result is consistent with the previously reported works[46-48]. The reason is that the calculated buckling energy (deformation energy) for this configuration is less than other considered configurations (see Fig. S2). Lower buckling energy means less energy is needed to distort the graphene plane. Bader charge analysis of oxidized graphene shows more negative charge on O atoms bound to same side of graphene sheet (see Fig. S2). This indicates

that the oxidized graphene with O atoms bound to same side of graphene sheet will be less stable due to charge repulsion between neighboring O atoms. In contrast, the O atoms are separated by graphene layer in oxidized graphene with O atoms bound to opposite sides of graphene sheet. It is evident that there will be less charge repulsion between O atoms which makes this configuration more stable. We have also studied the third O atom adsorption based on the most favorable adsorption sites for the second O atom adsorption. The calculated highest binding energy for third O atom adsorption is -3.18eV and preferred armchair orientation (see Fig. S3i). The calculated relative energy of graphene with epoxy chain (four epoxy groups are considered here) along armchair (both sides), armchair (same side) and zigzag (same side) orientations is 0.00, 0.44, and 0.88 eV, respectively. This suggests that the formation of epoxy chain is energetically most preferred along the armchair orientation but on different sides of graphene sheet (Fig. 2a). We also observe that the formation of two epoxy groups on the same side of graphene sheet prefers armchair orientation as compared to zigzag one (Fig. S2c). However, the formation of armchair epoxy chain on the same side of graphene sheet is energetically less favorable as compared to the zigzag orientation (Fig. 2a).

In addition, we have investigated the oxidative cutting of graphene via formation of carbonyl pair for armchair epoxy chain (Fig. 3) based on the mechanism proposed by Li et al[35]. The formation of epoxy pair breaks the C-C bond and forms a four-member ring (Fig. 3b) which is under high strain. The epoxy pair is converted to carbonyl pair to stabilize the oxidized graphene by releasing the high ring strain. The binding energy of O atom to form an epoxy pair

along armchair (Fig. 3a-b) and zigzag orientations (Fig. S4a-b) is -2.75 and -3.32 eV, respectively. This suggests that the graphene with epoxy pair along armchair orientation is energetically less stable than zigzag orientation. This is the reason that the conversion of armchair epoxy pair to carbonyl pair is much easier than zigzag epoxy pair (see Fig. 3 and S4c). Our theoretical calculations show that experimental design which allows the oxidation of graphene to happen at both sides of graphene sheet can generate GNRs and GQDs with dominantly armchair edges. However, to achieve oxidation at both sides of graphene experimentally one should use free graphene sheet. The both sides oxidation of single layer graphene has already been demonstrated experimentally by Liu et al[49].

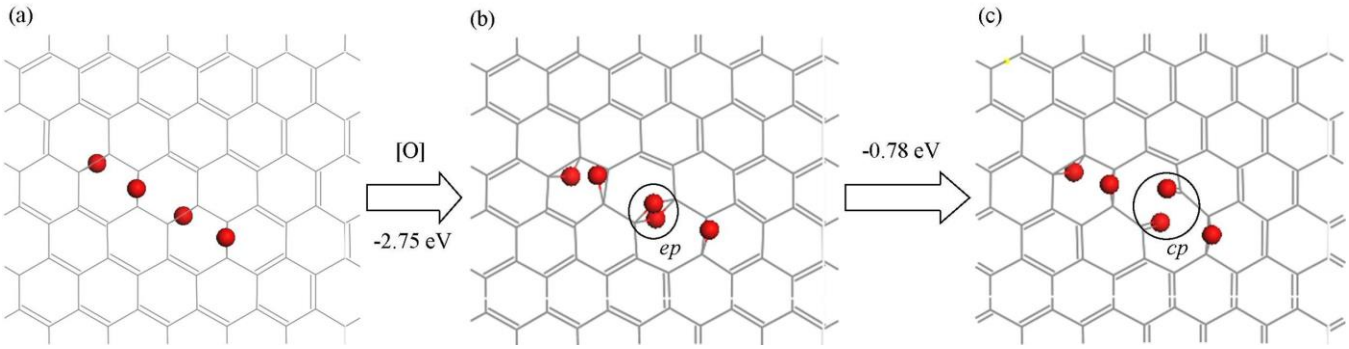

Fig. 3 Structure of graphene with (a) armchair epoxy chain, (b) epoxy pair, **ep** and (c) carbonyl pair, **cp**.

Oxidation at basal plane of strained graphene

Ma et al. in 2014 have proposed a potential experimental route to apply external tensile strain to graphene sheet and showed that external tensile strain on graphene makes the formation of epoxy chain energetically more favorable depending on the direction of applied strain.[36] The

applied strain breaks the symmetry of graphene and allows epoxy chain to form in a particular orientation. To investigate the effect of external strain on epoxy chain formation on graphene sheet we have applied both compressive and tensile strains. The applied strain is calculated according to the expression $(L - L_0)/L_0$, where L is the lattice constant of strained graphene along the strain direction, and L_0 is the equilibrium lattice constant of relaxed graphene along the strain direction. By convention, the tensile strain is positive and compressive strain is negative. We have applied strain in four directions with θ = 0, 30, 60 and 90° as shown in Fig. 4 (θ is the angle between epoxy chain and strain direction). The formation of epoxy chain on graphene sheet becomes more favorable when applying both tensile and compressive strains (Fig. 5). This can be explained by the elongation or contraction of C-C bonds oriented along applied strain directions. The formation of armchair epoxy chain becomes more favorable (indicated by more negative binding energy) when the compressive strain is applied at θ = 30° direction as compared to three other directions. In contrast, the formation of zigzag epoxy chain becomes more favorable when the strain is applied at θ = 90° as compared to other directions. This is because the application of compressive strain will contract the C-C bonds (along the applied strain directions) and thus will increase the C-C repulsion. To overcome this C-C repulsion the plane of graphene will be more susceptible to deform. Thus, less buckling energy is required to deform the graphene plane when the O atom is adsorbed on strained graphene and makes the formation of epoxy chain more favorable than on unstrained graphene. Our calculations reveal that when compressive strain is applied along armchair direction of graphene sheet, the formation of epoxy

chain is preferential along zigzag orientation. However, the formation of epoxy chain is observed along armchair orientation (θ = 30°) when compressive strain is applied along zigzag direction of graphene sheet. In addition, formation of zigzag epoxy chain under compressive strain is energetically most favorable as compared to armchair epoxy chain. We conclude here that by engineering the strain on graphene the orientation of epoxy chain formation can be controlled i.e., the edges of GNRs and GQDs. Since single-walled carbon nanotubes (SWNTs) can be seen as graphene sheet applied with higher strain, Guo et al. also found the similar result using oxidation cutting on SWNTs to get zigzag edges.[50]

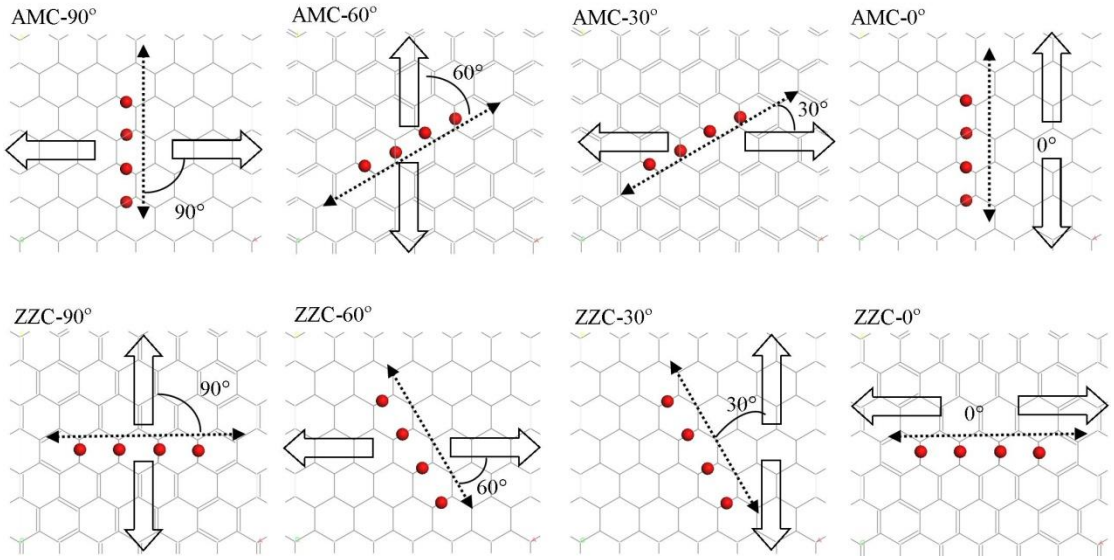

Fig. 4 Applied strain direction and epoxy chain formation direction.

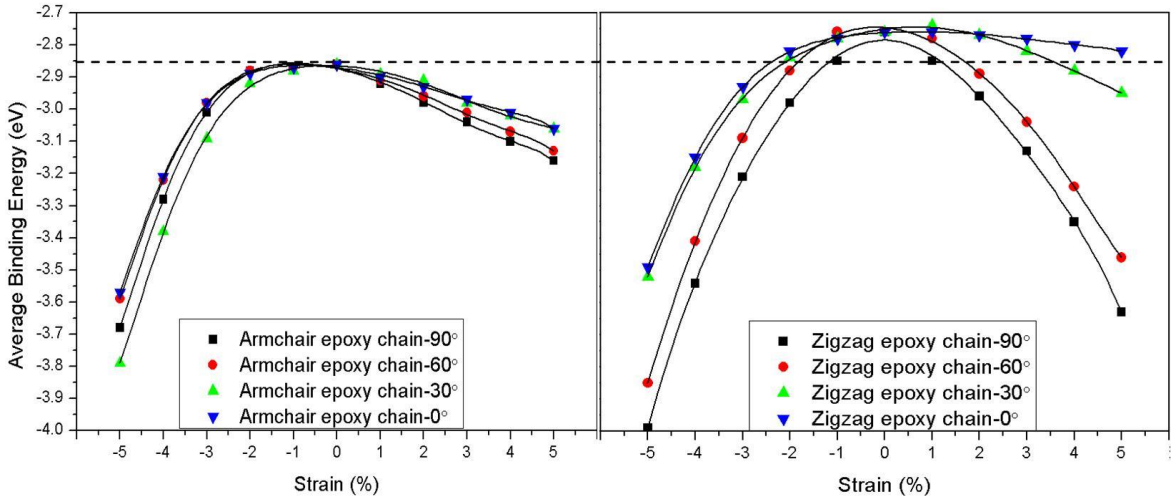

Fig. 5 Average binding energy of O atoms adsorption on graphene as a function of applied compressive and tensile strain.

Oxidation at the edges of graphene

We now consider the oxidation of graphene sheet at graphene edge considering both armchair (Fig. 1b) and zigzag (Fig. 1c) types. Binding energy of O atom at zigzag and armchair edge is -3.19 and -3.61 eV, respectively, which is much greater than binding at middle part of graphene sheet (-2.41 eV). For subsequent oxidation we have considered both edge and basal plane near the graphene edge for O atoms adsorption (Fig. 6). We observe that the epoxy pair formation at edge is more favorable than middle part of graphene sheet (Fig 6). Similar to the oxidation at middle part of graphene the formed epoxy pair is converted to carbonyl pair as shown in Fig. 6. We conclude that the oxidation of graphene sheet at edge is most favorable, when the edges of graphene are fully oxidized then the oxidation proceeds at the basal planes near edges. Similar to middle part of graphene, epoxy chair formation near graphene edge along

armchair orientation is energetically more favorable (Fig. 2b-c) as compared to zigzag orientation irrespective of graphene edge type (graphene with armchair or zigzag edge). The formation of zigzag epoxy chain become most favorable when compressive strain is applied along armchair direction of graphene sheet (Fig. S6). We reveal here that whether the oxidation of graphene sheet initiated at middle or edge of graphene, the formation of epoxy chain along armchair orientation is most preferable. Moreover, formation of zigzag epoxy chain becomes energetically most favorable when compressive strain is applied along the armchair direction of graphene sheet.

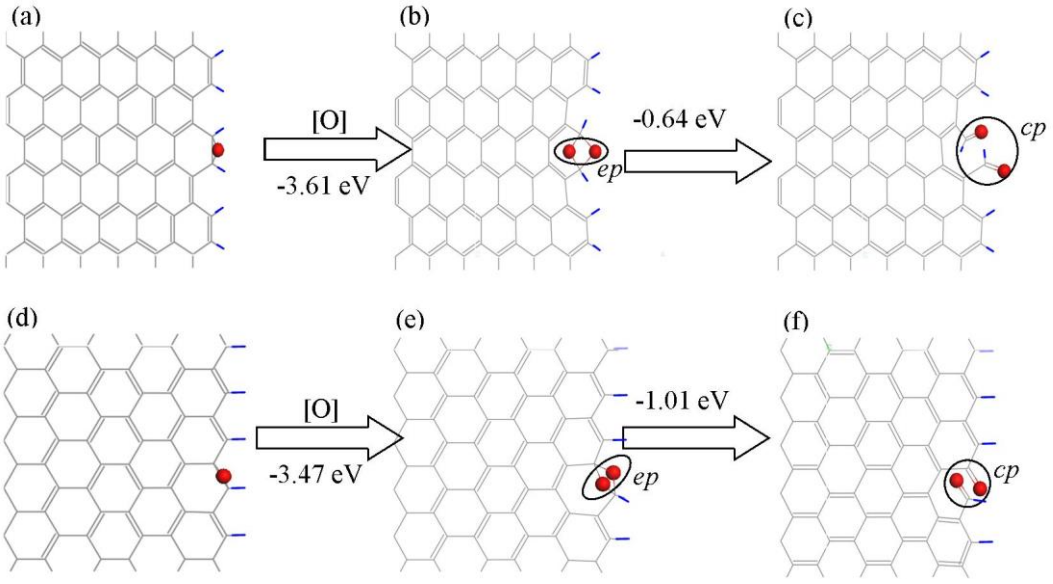

Fig. 6 Structure of armchair graphene edge with (a) epoxy group, (b) epoxy pair, ep and (c) carbonyl pair, cp; zigzag graphene edge with (a) epoxy group, (b) epoxy pair, ep and (c) carbonyl pair, cp.

Both oxidation of substrate bound graphene and free graphene sheet have been demonstrated experimentally. In our present study we have modelled the oxidation of graphene sheet on same and both sides of graphene sheet. The results obtained from the oxidation on same side of graphene can be used to understand the oxidation mechanism of substrate bound graphene while the oxidation on both sides of graphene can be used for the oxidation of free graphene sheet. We reveal that the oxidation on same side of strained graphene is energetically favorable than both sides and preferred to form epoxy chain along zigzag orientations. Our study shows that zigzag edges can be controlled by oxidizing substrate bound graphene under application of strain while the armchair edges can be controlled by oxidizing free graphene sheets.

Oxygen diffusion through graphene sheet

The oxidation at both sides of graphene sheets can be envisioned by oxidizing the single layer graphene. One possible way to observe the oxidation at both sides of graphene in substrate bound graphene or in graphite is the migration (diffusion) of O atom(s) through the graphene sheet (i.e., perpendicular to graphene plane). To understand the O atom diffusion through the graphene sheet, we have calculated the O atom diffusion barriers using the climbing-image nudged elastic band (CI-NEB) method[51-52]. Here, we consider the diffusion in both pure and oxidized graphene sheet. The calculated diffusion paths and potential energy curves along the diffusion paths are shown in Fig. 7.

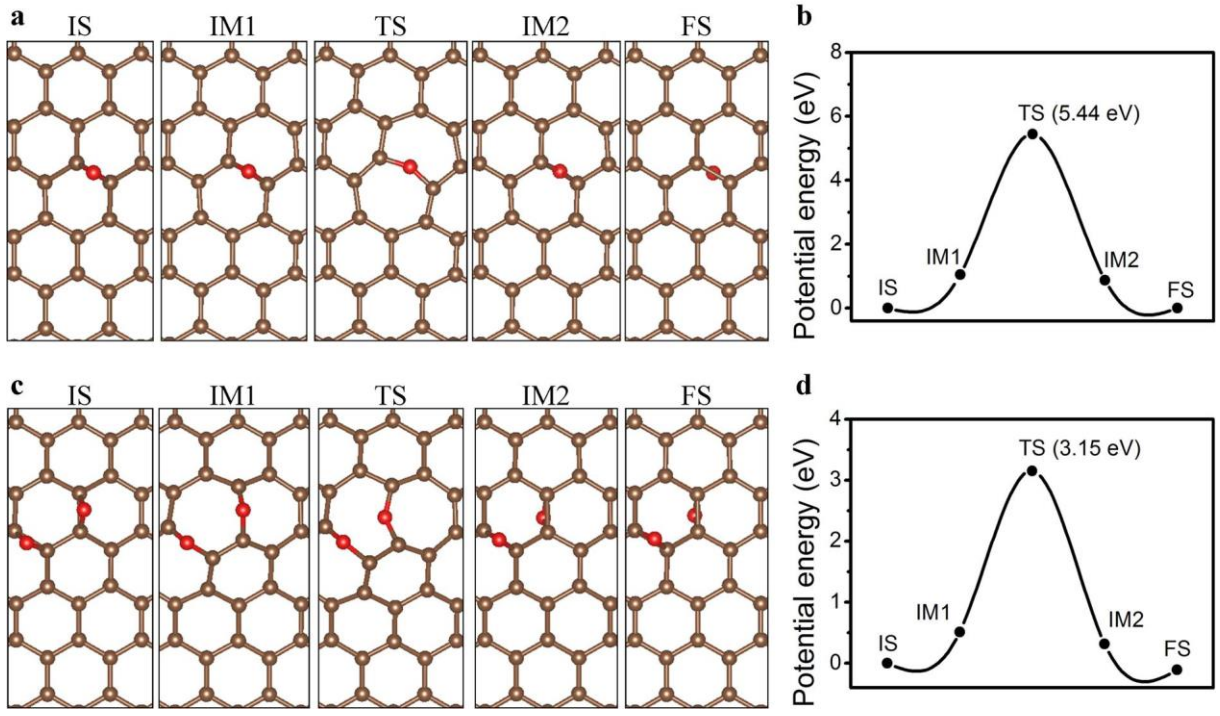

Fig. 7. The O atom diffusion path through (a) pure and (c) oxidized graphene sheet (only the relevant parts near O atom diffusion are shown). Calculated potential energy curves for (b) pure and (d) oxidized graphene along the diffusion path. The solid line in panel b and d is given to guide the eyes. IS, IM, TS and FS indicate initial, intermediate, transition and final state, respectively. First and last picture in panel a and c are stating (IS) and end (FS) point of the diffusion process. The potential energy curves are calculated at 3 NEB images: image 1 (IM1), 2 (TS) and 3 (IM2).

The calculated O atom diffusion barriers through the pure graphene and oxidized graphene are 5.44 and 3.15 eV. This suggests that the presence of pre-adsorbed O atoms lower the diffusion barrier. However, the O atom diffusion barriers through the pure and oxidized graphene

are much higher suggesting that the O atom diffusion through the graphene sheet is more unlikely to happen.

4 Conclusions

In conclusion, we have performed systematic study of graphene oxidation using DFT calculations. The oxidation at graphene edge is energetically more favorable as compared to middle part of graphene. Irrespective of binding sites on graphene, adsorption of O atoms leads to formation of armchair epoxy chain considering oxidation at both sides of graphene, which can be used to understand the oxidation cutting of graphene on substrate free condition. However, zigzag epoxy chain is formed when oxidation is considered on same side of graphene sheet. In addition, application of strain on graphene increases the binding affinity of O atoms with graphene. The orientation of epoxy chain formation on graphene changes from armchair to zigzag under applied compressive strain along armchair orientation of graphene sheet. The calculated high O atom diffusion barriers through the pure graphene and oxidized graphene indicated that O atom diffusion through the graphene sheet is unfavorable.

Our calculations reveal that by manipulating the experimental conditions and strain on graphene, the edges of GNRs and GQDs can be engineered.

Acknowledgements

This work was supported by the Singapore Ministry of Education under an AcRF Tier 2 grant

(MOE2014-T2-1-003).

Notes and references

1. K. S. Novoselov, A. K. Geim, S. V. Morozov, D. Jiang, Y. Zhang, S. V. Dubonos, I. V. Grigorieva and A. A. Firsov, *Science*, 2004, **306**, 666-669.
2. X. Wang, Y. Ouyang, X. Li, H. Wang, J. Guo and H. Dai, *Phys. Rev. Lett.*, 2008, **100**, 206803.
3. F. Schedin, A. K. Geim, S. V. Morozov, E. W. Hill, P. Blake, M. I. Katsnelson and K. S. Novoselov, *Nat Mater*, 2007, **6**, 652-655.
4. X. Dong, Q. Long, J. Wang, M. B. Chan-Park, Y. Huang, W. Huang and P. Chen, *Nanoscale*, 2011, **3**, 5156-5160.
5. E. U. Stützel, M. Burghard, K. Kern, F. Traversi, F. Nichele and R. Sordan, *Small*, 2010, **6**, 2822-2825.
6. Y. Dong, C. Chen, X. Zheng, L. Gao, Z. Cui, H. Yang, C. Guo, Y. Chi and C. M. Li, *J. Mater. Chem.*, 2012, **22**, 8764-8766.
7. Q. Liu, B. Guo, Z. Rao, B. Zhang and J. R. Gong, *Nano Lett.*, 2013, **13**, 2436-2441.
8. X. T. Zheng, A. Than, A. Ananthanaraya, D.-H. Kim and P. Chen, *ACS Nano*, 2013, **7**, 6278-6286.
9. X. Wu, F. Tian, W. Wang, J. Chen, M. Wu and J. X. Zhao, *Journal of Materials Chemistry C*, 2013, **1**, 4676-4684.
10. H. Sun, L. Wu, W. Wei and X. Qu, *Materials Today*, 2013, **16**, 433-442.
11. A. Ananthanarayanan, X. Wang, P. Routh, B. Sana, S. Lim, D.-H. Kim, K.-H. Lim, J. Li

and P. Chen, *Advanced Functional Materials*, 2014, **24**, 3021-3026.

12. W.-W. Liu, Y.-Q. Feng, X.-B. Yan, J.-T. Chen and Q.-J. Xue, *Advanced Functional Materials*, 2013, **23**, 4111-4122.

13. Y. Li, Y. Hu, Y. Zhao, G. Shi, L. Deng, Y. Hou and L. Qu, *Adv. Mater.*, 2011, **23**, 776-780.

14. V. Gupta, N. Chaudhary, R. Srivastava, G. D. Sharma, R. Bhardwaj and S. Chand, *Journal of the American Chemical Society*, 2011, **133**, 9960-9963.

15. K. A. Ritter and J. W. Lyding, *Nat Mater*, 2009, **8**, 235-242.

16. Y.-W. Son, M. L. Cohen and S. G. Louie, *Phys. Rev. Lett.*, 2006, **97**, 216803.

17. M. A. Sk, A. Ananthanarayanan, L. Huang, K. H. Lim and P. Chen, *Journal of Materials Chemistry C*, 2014, **2**, 6954-6960.

18. Z. Chen, Y.-M. Lin, M. J. Rooks and P. Avouris, *Physica E: Low-dimensional Systems and Nanostructures*, 2007, **40**, 228-232.

19. M. Y. Han, B. Özyilmaz, Y. Zhang and P. Kim, *Phys. Rev. Lett.*, 2007, **98**, 206805.

20. C. Stampfer, J. Güttinger, F. Molitor, D. Graf, T. Ihn and K. Ensslin, *Applied Physics Letters*, 2008, **92**, 012102.

21. R. Yang, L. Zhang, Y. Wang, Z. Shi, D. Shi, H. Gao, E. Wang and G. Zhang, *Adv. Mater.*, 2010, **22**, 4014-4019.

22. B. Krauss, P. Nemes-Incze, V. Skakalova, L. P. Biro, K. v. Klitzing and J. H. Smet, *Nano Lett.*, 2010, **10**, 4544-4548.

23. Z.-S. Wu, W. Ren, L. Gao, B. Liu, J. Zhao and H.-M. Cheng, *Nano Res.*, 2010, **3**, 16-22.

24. Y. Guo and W. Guo, *The Journal of Physical Chemistry C*, 2011, **115**, 20546-20549.

25. L. Ci, Z. Xu, L. Wang, W. Gao, F. Ding, K. Kelly, B. Yakobson and P. Ajayan, *Nano Res.*, 2008, **1**, 116-122.

26. S. S. Datta, D. R. Strachan, S. M. Khamis and A. T. C. Johnson, *Nano Lett.*, 2008, **8**, 1912-1915.

27. D. Pan, J. Zhang, Z. Li and M. Wu, *Adv. Mater.*, 2010, **22**, 734-738.

28. X. Li, X. Wang, L. Zhang, S. Lee and H. Dai, *Science*, 2008, **319**, 1229-1232.

29. S. Fujii and T. Enoki, *Journal of the American Chemical Society*, 2010, **132**, 10034-10041.

30. X. Gao, L. Wang, Y. Ohtsuka, D.-e. Jiang, Y. Zhao, S. Nagase and Z. Chen, *Journal of the American Chemical Society*, 2009, **131**, 9663-9669.

31. J.-L. Li, K. N. Kudin, M. J. McAllister, R. K. Prud'homme, I. A. Aksay and R. Car, *Phys. Rev. Lett.*, 2006, **96**, 176101.

32. T. Szabó, O. Berkesi, P. Forgó, K. Josepovits, Y. Sanakis, D. Petridis and I. Dékány, *Chem. Mat.*, 2006, **18**, 2740-2749.

33. T. Sun and S. Fabris, *Nano Lett.*, 2011, **12**, 17-21.

34. J. T. Paci, T. Belytschko and G. C. Schatz, *The Journal of Physical Chemistry C*, 2007, **111**, 18099-18111.

35. Z. Li, W. Zhang, Y. Luo, J. Yang and J. G. Hou, *Journal of the American Chemical Society*, 2009, **131**, 6320-6321.

36. L. Ma, J. Wang and F. Ding, *Angewandte Chemie International Edition*, 2012, **51**, 1161-1164.

37. J. P. Perdew, K. Burke and M. Ernzerhof, *Phys. Rev. Lett.*, 1996, **77**, 3865-3868.

38. G. Kresse and J. Hafner, *Phys. Rev. B*, 1993, **48**, 13115-13118.

39. G. Kresse and J. Furthmuller, *Phys. Rev. B*, 1996, **54**, 11169-11186.

40. G. Kresse and J. Furthmüller, *J. Comp. Mat. Sci.*, 1996, **6**, 15-50.

41. P. E. Blochl, *Phys. Rev. B*, 1994, **50**, 17953.

42. G. Kresse and D. Joubert, *Phy. Rev. B*, 1999, **59**, 1758-1775.

43. H. J. Monkhorst and J. D. Pack, *Phy. Rev. B*, 1976, **13**, 5188-5192.

44. M. J. McAllister, J.-L. Li, D. H. Adamson, H. C. Schniepp, A. A. Abdala, J. Liu, M. Herrera-Alonso, D. L. Milius, R. Car, R. K. Prud'homme and I. A. Aksay, *Chem. Mat.*, 2007, **19**, 4396-4404.

45. H. C. Schniepp, J.-L. Li, M. J. McAllister, H. Sai, M. Herrera-Alonso, D. H. Adamson, R. K. Prud'homme, R. Car, D. A. Saville and I. A. Aksay, *The Journal of Physical Chemistry B*, 2006, **110**, 8535-8539.

46. L. Wang, Y. Y. Sun, K. Lee, D. West, Z. F. Chen, J. J. Zhao and S. B. Zhang, *Phys. Rev. B*, 2010, **82**, 161406(R).

47. N. Lu, D. Yin, Z. Li and J. Yang, *J. Phys. Chem. C*, 2011, **115**, 11991-11995.

48. J.-A. Yan and M. Y. Chou, *Phys. Rev. B*, 2010, **82**, 125403.

49. L. Liu, S. Ryu, M. R. Tomasik, E. Stolyarova, N. Jung, M. S. Hybertsen, M. L.

Steigerwald, L. E. Brus and G. W. Flynn, *Nano Lett.*, 2008, **8**, 1965-1970.

50. Y. Guo, L. Jiang and W. Guo, *Phys. Rev. B*, 2010, **82**, 115440.

51. G. Henkelman, B.P. Uberuaga, H. Jónsson, *J. Chem. Phys.*, 2000, 113, 9901.

52. G. Henkelman, H. Jónsson, *J. Chem. Phys.*, 2000, 113, 9978.

Table of Contents

DFT calculations reveal that the edges of GNRs and GQDs can be controlled by manipulating the experimental conditions and external strain on graphene sheet.